

## Dat Com and Missile Dat Com Results

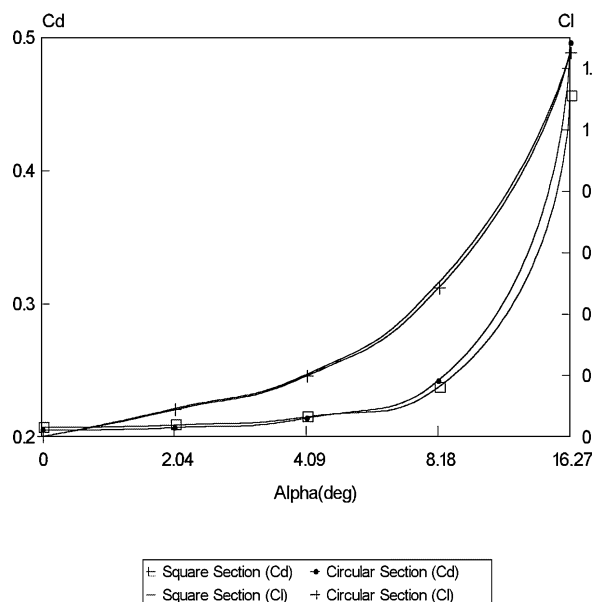


Fig. 6 Comparison of drag and lift coefficients for square and circular bodies (semi-empirical results).

### Conclusions

In order to investigate the effects of the shape of the cross-sections, two different cases, circular and square with round corners, were studied in this work using computational and semi-empirical methods. The results that are mainly in the form of aerodynamic coefficients show better aerodynamic performance for the square section missile at different angles of attack. Because the square body, in comparison with the circular one, causes more lift and a bit less drag. It is noticeable that although the friction drag is more for the square case due to its larger surface area, the overall drag of the square case is somehow smaller than that of the circular case.

### References

- Jackson, C. M., and Sawyer, W. C., "Bodies with Non-Circular Cross-Sections and Bank-to-Turn Missiles," *Tactical Missile Aerodynamics: General Topics*, edited by M. J. Hemsch, Vol. 141, Progress in Astronautics and Aeronautics, AIAA, Washington, DC, 1991, pp. 365–389.
- Graves, E. B., "Aerodynamic Characteristics of a Mono-Planar Missile Concept with Bodies of Circular and Elliptical Cross-Sections," NASA TM-74079, Dec. 1977.
- Sharma, R. K., "Experimental Aerodynamic Characteristics of Elliptical Bodies with Variation in Ellipticity Ratio," *Proceedings of the 18th AIAA Applied Aerodynamics Conference and Exhibit*, Denver, CO, USA, Aug. 2000.
- Sigal, A., and Lapidot, E., "The Aerodynamic Characteristics of Configurations Having Bodies with Square, Rectangular, and Circular Cross-Sections at a Mach Number of 0.75," *AIAA Atmospheric Flight Mechanics Conference*, Monterey, CA, Aug. 1987.
- Nielsen, J. N., "Problems Associated with the Aerodynamic Design of Missile Shapes," *Proceedings of the Second Symposium on Numerical and Physical Aspects of Aerodynamic Flows*, edited by T. Cebeci, California State Univ., Springer, CA, USA, Jan. 1983.
- Schneider, W., "Experimental Investigation of Bodies with Non-Circular Cross-Section in Compressible Flow," *Symposium on Missile Aerodynamics*, AGARD-CP-336, Trondheim, Norway, 20–22 Sept. 1982, pp. 19-1–19-15.
- Daniel, D. C., Yechout, T. R., and Zollars, G. J., "Experimental Aerodynamic Characteristics of Missiles with Square Cross-Sections," *Journal of Spacecraft and Rockets*, Vol. 19, No. 2, 1982.
- "FLUENT 5 User's Guide," FLUENT Inc., Lebanon, New Jersey, July 1998.
- Birch, T. J., Wrisdale, I. E., and Prince, S. A., "CFD Predictions of Missile Flow-Fields," *Proceedings of the 18th AIAA Applied Aerodynamics Conference and Exhibit*, Denver, CO, USA, Aug. 2000.
- Bulbeck, C. J., Morgan, J., and Fairlie, B. D., "RANS Computations of High-Incidence Missile Flow Using Hybrid Meshes," *Proceedings of the*

18th AIAA Applied Aerodynamics Conference and Exhibit, Denver, CO, USA, Aug. 2000.

<sup>11</sup>Keimasi, M. R., and Taeibi-Rahni, M., "Numerical Simulation of Jets in a Cross-Flow Using Different Turbulence Models," *AIAA Journal*, Vol. 39, No. 12, 2001, pp. 2268–2277.

<sup>12</sup>Mani, M., and Khajehfard, A., "Aerodynamic Characteristics of Bodies with Square, Elliptic and Circular Cross-Sections," *Proceedings of the 18th AIAA Applied Aerodynamics Conference and Exhibit*, Aug. 2000.

<sup>13</sup>"The USAF Stability and Control Digital DatCom," The Air Force Wright Aeronautical Lab., AFWAL/FIGC, McDonnell Douglas Astronautics Co., OH, April 1979.

<sup>14</sup>Vukelich, S., R., Stoy, S. L., and Moore, M. E., "The USAF Automated Missile DatCom," AFWAL-TR-86-3091, McDonnell Douglas Missile Systems Co., 1986.

## Incorrectness of the $k$ Method for Flutter Calculations

Mayuresh J. Patil\*

Virginia Polytechnic Institute and State University,  
Blacksburg, Virginia 24061

Rudolph N. Yurkovich†

The Boeing Company, St. Louis, Missouri 63166

and

Dewey H. Hodges‡

Georgia Institute of Technology,  
Atlanta, Georgia 30332-0150

### Introduction

IT has been appreciated by aeroelasticians for many years that results from the  $V$ - $g$  or  $k$  method of flutter analysis can be difficult to interpret or even misleading.<sup>1–3</sup> The purpose of the present Note is to consider this difficulty with the  $k$  method in an especially simple setting, that is, with steady-flow aerodynamics. As Pines<sup>4</sup> showed many years ago in a different context, the use of highly simplified aerodynamics can be especially illuminating. In the special case of steady-flow aerodynamics and zero structural damping, the principal result of the present Note shows one way that the  $V$ - $g$  or  $k$  method can lead to difficulties. For this special case, a particularly clear understanding of the nature of these difficulties can be obtained. This Note adds a modest but new and, the authors believe, helpful addition to the rich literature on this perplexing issue.

It is well known that  $k$  and  $p$  methods of calculating flutter speeds are quite different.<sup>5</sup> It is frequently assumed that both methods calculate the same flutter point because at zero damping (sinusoidal motion) both the methods are mathematically the same.<sup>6</sup> Nevertheless, the authors have come across cases in which the flutter speed, as defined by the speed after which the damping measure is negative (i.e., the real part of the eigenvalue is positive in  $p$  method, and artificial damping is positive in  $k$  method) or the speed at which frequency coalescence occurs, is predicted differently by the two methods. The inconsistency of the  $k$  method in predicting the flutter speed can be directly observed in systems without viscous damping (i.e., without forces proportional to velocity) in either the structural or aerodynamic operators. Such a system is neutrally stable for all

Received 26 March 2003; revision received 9 September 2003; accepted for publication 25 November 2003. Copyright © 2004 by the authors. Published by the American Institute of Aeronautics and Astronautics, Inc., with permission. Copies of this paper may be made for personal or internal use, on condition that the copier pay the \$10.00 per-copy fee to the Copyright Clearance Center, Inc., 222 Rosewood Drive, Danvers, MA 01923; include the code 0021-8669/04 \$10.00 in correspondence with the CCC.

\*Assistant Professor, Department of Aerospace and Ocean Engineering, Member AIAA.

†Boeing Technical Fellow, Fellow AIAA.

‡Professor, School of Aerospace Engineering, Fellow AIAA.

preflutter speeds. The flutter speed is determined as the speed at which the system jumps from neutral stability to instability. Thus, the mathematical uniqueness inherent in systems that evolve from a state of stability to one of instability via a single point of neutral stability is lost. It is the aim of this Note to present this seemingly unlikely finding and use this simple example to study the  $k$  method.

The kind of aeroelastic system implied by the preceding restrictions is one in which a steady-flow aerodynamic model is assumed. In such systems the aerodynamic force contribution depends only on the instantaneous geometric angle of attack. The use of steady-flow aerodynamics for flutter problems constitutes a relatively simplistic approximation, but such simplified models have been used to provide an elementary explanation of the flutter problem, as well as physical insight into it.<sup>4,7</sup> In particular, the steady-flow aerodynamic model is helpful in illustrating the phenomenon of coalescence. Note that it is not the purpose here to justify the assumption of steady-flow aerodynamics; rather, it is to use this special case to gain insight into different flutter solution procedures. With steady-flow aerodynamics, the stability of the system can be easily and directly calculated by the  $p$  method. The  $k$  method is not needed for the simple system under consideration, but one can represent the problem in the  $k$ -method form. This simple system highlights some differences in the methods that are not easily observed with complex systems.

### The Problem

The aeroelastic system under consideration is a typical airfoil section model. Figure 1 shows the airfoil with relevant nomenclature. Only steady-flow aerodynamic forces are considered (thus affecting only the stiffness of the system). The system equations of motion can be written in nondimensional form as<sup>8</sup>

$$\begin{bmatrix} 1 & x_\theta \\ x_\theta & r^2 \end{bmatrix} \begin{Bmatrix} \ddot{h} \\ \ddot{\theta} \end{Bmatrix} + \begin{bmatrix} 1 & 0 \\ 0 & \sigma^2 r^2 \end{bmatrix} \begin{Bmatrix} \dot{h} \\ \dot{\theta} \end{Bmatrix} = \begin{bmatrix} 0 & -\frac{2V^2}{\mu} \\ 0 & \frac{2V^2}{\mu} \left( \frac{1}{2} + a \right) \end{bmatrix} \begin{Bmatrix} h \\ \theta \end{Bmatrix} \quad (1)$$

where the nondimensional parameters in the preceding equation can be related to the actual system parameters as  $\bar{h}/b$ ,  $r^2 = I_p/m b^2$ ,  $\sigma = \omega_\theta/\omega_h$ ,  $\omega_\theta^2 = k_\theta/I_p$ ,  $\omega_h^2 = k_h/m$ ,  $\mu = m/\rho_\infty \pi b^2$ , and  $V = U_\infty/b\omega_h$ , where  $h$  is the plunge,  $\theta$  is the pitch,  $b$  is the semichord,  $m$  and  $I_p$  are the mass and moment of inertia of the airfoil,  $k_h$  and  $k_\theta$  are the plunge and pitch spring stiffnesses,  $\rho_\infty$  is the freestream density, and  $U_\infty$  is the flight speed. The nondimensional parameter  $x_\theta = e - a$ , where  $e$  and  $a$  are nondimensional offsets from the midchord to the center of gravity and to the elastic axis, respectively, as shown in Fig. 1, and a nondimensional time given by  $\tau = \omega_h t$  is used. For the present numerical calculations the parameters chosen are  $\sigma = \sqrt{2}$ ,  $r^2 = \frac{1}{3}$ ,  $a = 0$ ,  $x_\theta = 0.25$ , and  $\mu = 200$ .

### Flutter Solution: $p$ Method

The equation of motion of the aeroelastic system as just described is converted to an eigenvalue problem by letting  $\bar{h} = \hat{h}e^{\lambda t}$

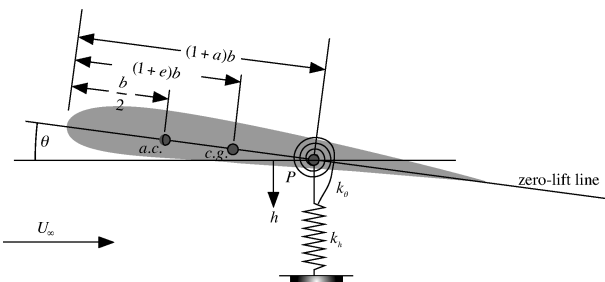


Fig. 1 Airfoil undergoing pitch-plunge motion.

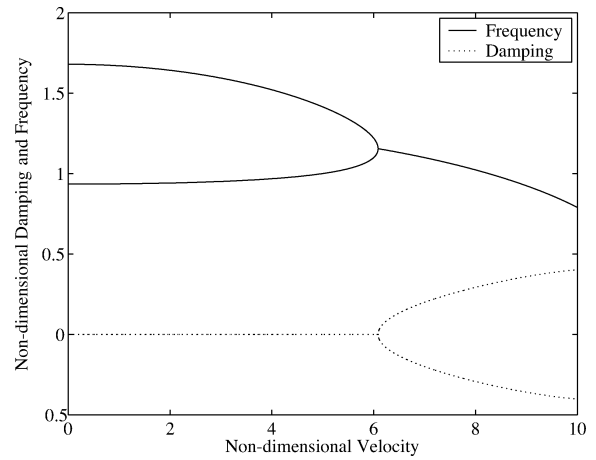


Fig. 2 Flutter solution using the  $p$  method.

and  $\theta = \hat{\theta}e^{\lambda t}$ , thus leading to an eigenvalue problem of the form

$$\lambda^2 \begin{Bmatrix} \hat{h} \\ \hat{\theta} \end{Bmatrix} = \begin{bmatrix} 1 & x_\theta \\ x_\theta & r^2 \end{bmatrix}^{-1} \begin{bmatrix} -1 & -\frac{2V^2}{\mu} \\ 0 & -\sigma^2 r^2 + \frac{2V^2}{\mu} \left( \frac{1}{2} + a \right) \end{bmatrix} \begin{Bmatrix} \hat{h} \\ \hat{\theta} \end{Bmatrix} \quad (2)$$

The preceding eigenvalue problem can be solved at various speeds to obtain  $\lambda$ . The imaginary and real parts of  $\lambda$  give the nondimensional frequency and damping of the system modes, respectively.

Figure 2 shows the nondimensional frequency and damping variation of the system as a function of  $V$ , the nondimensional flight speed. The nondimensional flutter speed is found to be  $V_F = 6.086$ , the nondimensional flutter frequency is 1.155, and the flutter reduced frequency is 0.1898.

### Flutter Solution: $k$ Method

The  $k$  method is based on the assumption of sinusoidal motion for the aeroelastic system. This assumption is usually needed because unsteady aerodynamic loads are available only for sinusoidal motions. The aerodynamic forces can then be represented in terms of the reduced frequency  $k$ . The eigenvalue problem is then obtained by addition of an artificial, stiffness-proportional damping (forces in phase with velocity) term so as to account for the imaginary part of the eigenvalues. The  $k$  method eigenvalue problem can be written as

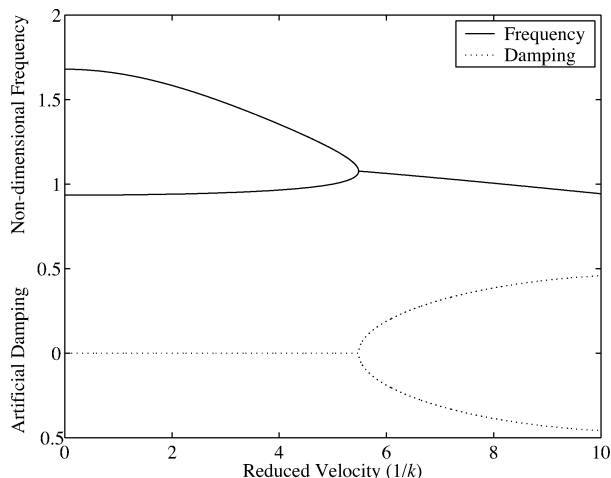
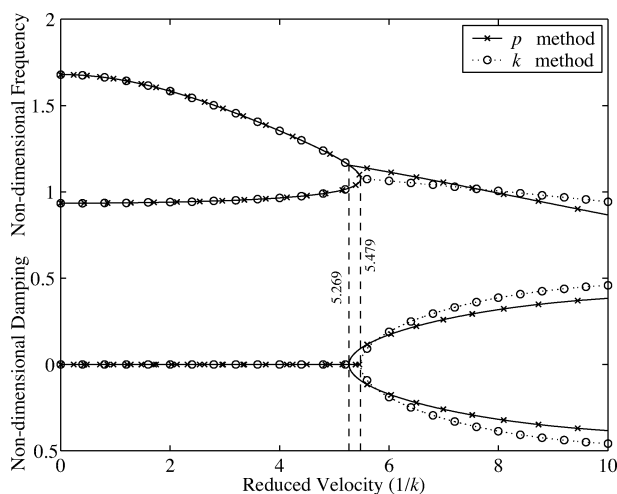
$$\frac{1 + ig}{\omega^2} \begin{Bmatrix} \hat{h} \\ \hat{\theta} \end{Bmatrix} = \begin{bmatrix} 1 & 0 \\ 0 & \sigma^2 r^2 \end{bmatrix}^{-1} \begin{bmatrix} 1 & x_\theta - \frac{2}{\mu k^2} \\ x_\theta & r^2 + \frac{2}{\mu k^2} \left( \frac{1}{2} + a \right) \end{bmatrix} \begin{Bmatrix} \hat{h} \\ \hat{\theta} \end{Bmatrix} \quad (3)$$

The eigenvalue problem can be solved at various values of reduced frequency  $k$  to obtain the nondimensional frequency  $\omega$  and artificial damping  $g$ . Thus the  $k$  method is set up to calculate the stiffness-proportional damping required to force the system response to be sinusoidal.

Figure 3 shows the nondimensional frequency and artificial damping as a function of reduced velocity ( $1/k$ ) obtained by using the  $k$  method. Using the  $k$  method, the flutter instability is predicted at a reduced velocity of 5.479 and a non-dimensional flutter frequency of 1.077, corresponding to a nondimensional flutter speed of  $V_F = 5.901$ . This flutter speed is around 3% lower than that obtained by the  $p$  method. The flutter reduced velocity is higher than that determined from the  $p$  method.

### Discussion

Clearly the frequency coalescence solutions provided by the two methods are in disagreement. In what follows some explanations are provided for this discrepancy.

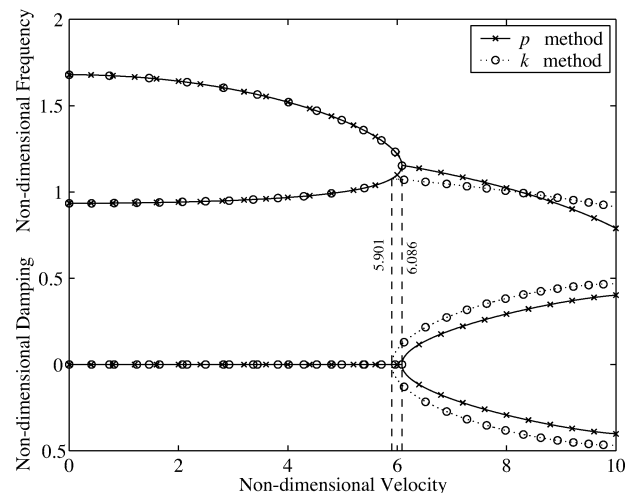
Fig. 3 Flutter solution using the  $k$  method.Fig. 4 Comparison of flutter solutions in  $k$  space.

#### Comparison of the Results in $k$ space

Figure 4 compares results for the nondimensional frequency and damping measures (the latter being the real part of the eigenvalue for the  $p$  method and the artificial damping for the  $k$  method) of the system obtained using the two methods. To do this, the results obtained by the  $p$  method are plotted as a function of reduced velocity. The transformation into  $k$  space can be accomplished by relating speed and the undamped frequency of the aeroelastic mode to the reduced velocity. Such a plot can also be graphically obtained by drawing radial lines on the  $p$  domain plot (which reflect lines of constant  $k$ ). The points at which these lines of constant  $k$  intersect the  $p$  method results give the aeroelastic roots for that  $k$ .

As can be seen, the  $p$  method predicts frequency coalescence at a lower reduced velocity as compared to the  $k$  method. Normally, when using the complete unsteady aerodynamic loads the damping is nonzero and positive for low speeds. The flutter point signifies the transition from a stable, damped response to an unstable response, given by the point of zero damping. Because for the zero-damping case both the solutions are equivalent, the same flutter speed is normally predicted. In the present case though, there is a curve of zero damping rather than a point of zero damping because the damping is zero for multiple reduced velocities (from zero to flutter). As expected, the same zero-damping curve is predicted by both the solutions, but the two solution procedures predict different points at which the curve enters the unstable regime.

The reason for the inability of the  $k$  method to predict the same frequency coalescence point as the  $p$  method predicts can now be seen graphically. The  $p$  method (plotted in the  $k$  domain) predicts four roots at reduced velocity ( $1/k$ ) range between 5.269 and 5.479. To predict a flutter point at the same reduced frequency, the  $k$  method

Fig. 5 Comparison of flutter solutions in  $p$  space.

would have to predict four modes as well. This is obviously not possible because only two roots per reduced velocity can be obtained for the two-degree-of-freedom system using the  $k$  method. In this range, the  $k$  method is constrained to predict the zero-damping solution. Thus, the roots that it will not predict are the postflutter roots.

#### Comparison of Results in the $p$ Domain

To further explain the anomaly just described, the  $k$  solution is compared to the  $p$  solution in the  $p$  domain (i.e., plotting results with respect to the nondimensional flight speed). The results obtained by the  $k$  method can be transformed to  $p$  space by relating the reduced frequency and undamped frequency of the aeroelastic mode to the speed. Figure 5 shows the frequencies and damping measure of the system obtained by both methods as a function of the nondimensional speed. It is again clear that the  $k$  method predicts the same zero-damping solution curve as the  $p$  method but a lower nondimensional speed at which frequency coalescence occurs. Also the  $k$  method predicts four solutions at nondimensional speeds between 5.901 and 6.086, two on the zero-damping curve (different frequencies but zero damping) and two after frequency coalescence (same frequency but positive and negative damping).

To understand the solution given by the  $k$  method, one needs to understand the underlying assumptions of its solution methodology. The  $k$  method eigenvalue problem is posed such that if the eigenvalue is real then it denotes a frequency of the system. If, however, the eigenvalue is complex, then there is in general no connection between these complex eigenvalues and the actual eigenvalues of the system (i.e., those predicted by the  $p$  method). But the eigenvalues still do indicate some aspects of the system behavior, that is, the imaginary part of the eigenvalue gives the stiffness proportional damping to be applied to the system to make it neutrally stable.

The preceding explanation implies that the  $g$  predicted by the  $k$  method is the damping required to be added to the system for it to undergo simple harmonic oscillation (neutral stability). For nondimensional speeds between 5.901 and 6.086 (refer to Fig. 5), the  $k$  method predicts four roots for the two-degree-of-freedom system. Two roots have zero  $g$ , one has positive  $g$  and one has negative  $g$ . The two zero- $g$  roots imply that no structural damping is required to maintain simple harmonic motion; and, thus, it predicts that the system is neutrally stable. On the other hand, the positive- $g$  root implies that there exists a positive damping of a certain magnitude which, when added, makes the system neutrally stable. This then is usually taken to mean that if such a positive damping is not provided then the real system will be unstable. The last statement is the weak link in the interpretation of the  $k$  results. If a system needs damping to be neutrally stable, then it is in general not true that the system would be unstable without this damping.

To gain better insight into the actual behavior, a case of  $V = 6$  is chosen, which is in between the frequency coalescence points of

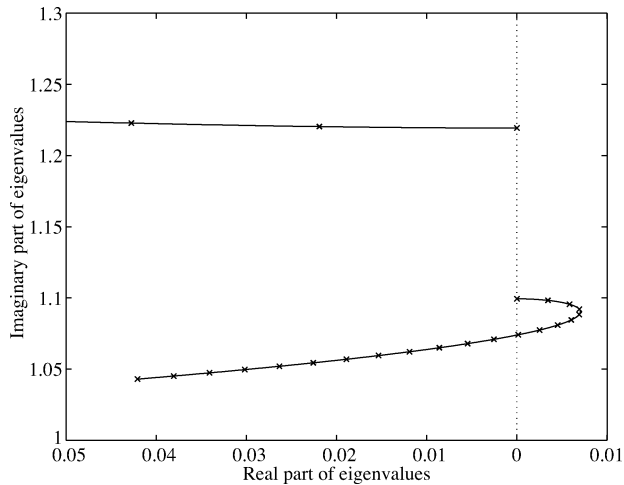


**Fig. 6** Effect of proportional damping on the stability characteristics of the airfoil.

the  $p$  and  $k$  solutions. For this case the system is neutrally stable (as predicted by the  $p$  method and ambiguously by the  $k$  method). Now stiffness-proportional viscous damping is added, and the system is solved using the  $p$  method. Figure 6 shows the change in the eigenvalues of the system with  $c$  (damping proportionality factor) ranging from  $c = 0$  to 0.2, with 0.01 increments in  $c$  denoted by the cross marks. Here it is clear that even for positive structural damping one of the roots becomes unstable for a while and then becomes stable. Hence, there exists a value of  $g$ , which, if added, causes the system to return to neutral stability. The  $k$  method does predict correctly this second value of  $c$  (apart from  $c = 0$ ) for which the system is neutrally stable. This insight provided by the  $k$  method is important because in realistic problems there is a distinct possibility of small structural damping where the  $k$  method accurately predicts the possibility of instability.

The reason for small stiffness-proportional damping to lead to destabilization of the system might be surprising at first, but such a destabilizing effect of damping has been shown in various previous works.<sup>9,10</sup> The instability of an aeroelastic system can be attributed to the extraction of energy from the flow.<sup>11</sup> The rate of energy extraction depends on the aeroelastic mode shape (phase relationship between the pitch and plunge). Now, addition of damping can help remove some energy from the structure, but it can also change the aeroelastic mode shape. This change in the mode shape can lead to an increase in the rate of energy extraction. If the increase in the rate of energy extraction as a result of the phase change caused by the added damping is more than the rate of energy removal as a result of damping, then the damping leads to an increase in the margin of instability.

### Conclusions

The  $p$  and  $k$  methods predict different frequency coalescence points (flutter speeds) for the problem considered, which is to say that the  $k$  method predicts an incorrect flutter speed. However, this has nothing to do with accuracy of either method. Instead, the methods provide solutions to different problems, and thus the solutions obtained from the methods have different interpretations. Because the primary interest is the flutter speed of the system, it is more relevant to consider the evolution of the system roots as a function of flight speed rather than reduced velocity. The point remains that both the methods have potential for insight into a given aeroelastic problem if the results are correctly interpreted.

### Acknowledgment

The authors thank Earl Dowell for his suggestions.

### References

<sup>1</sup>Fung, Y. C., *An Introduction to the Theory of Aeroelasticity*, Wiley, New York, 1955, Chap. 6.

<sup>2</sup>Bisplinghoff, R. L., and Ashley, H., *Principles of Aeroelasticity*, Wiley, New York, 1962, Chap. 6.

<sup>3</sup>Dowell, E. H. (ed.), *A Modern Course in Aeroelasticity*, 3rd ed., Kluwer Academic, Norwell, MA, 1995, Chap. 3.

<sup>4</sup>Pines, S., "An Elementary Explanation of the Flutter Mechanism," *Proceedings of the National Specialists Meeting on Dynamics and Aeroelasticity*, Inst. of the Aeronautical Sciences, Fort Worth, TX, 1958, pp. 52–58.

<sup>5</sup>Hassig, H. J., "An Approximate True Damping Solution of the Flutter Equation by Determinant Iteration," *Journal of Aircraft*, Vol. 8, No. 11, 1971, pp. 885–889.

<sup>6</sup>Rodden, W. P., and Bellinger, E. D., "Aerodynamic Lag Functions, Divergence, and the British Flutter Method," *Journal of Aircraft*, Vol. 19, No. 7, 1982, pp. 596–598.

<sup>7</sup>Hodges, D. H., and Pierce, G. A., *Introduction to Structural Dynamics and Aeroelasticity*, Cambridge Univ. Press, Cambridge, England, U.K., 2002, Chap. 4.

<sup>8</sup>Bisplinghoff, R. L., Ashley, H., and Halfman, R. L., *Aeroelasticity*, Addison Wesley Longman, Reading, MA, 1955, Chap. 9.

<sup>9</sup>Herrmann, G., and Jong, I.-C., "On the Destabilizing Effect of Damping in Nonconservative Elastic Systems," *Journal of Applied Mechanics*, Vol. 32, No. 3, 1965, pp. 592–597.

<sup>10</sup>Nissim, E., "Effect of Linear Damping on Flutter Speed. Part I: Binary Systems," *The Aeronautical Quarterly*, Vol. 16, May 1965, pp. 159–178.

<sup>11</sup>Patil, M. J., "From Fluttering Wings to Flapping Flight: The Energy Connection," *Journal of Aircraft*, Vol. 40, No. 2, 2003, pp. 270–276.

## Effects of Active and Passive Flow Control on Dynamic-Stall Vortex Formation

Lance W. Traub,\* Adam Miller,<sup>†</sup> and Othon Rediniotis<sup>‡</sup>  
Texas A&M University, College Station, Texas 77843-3141

### Introduction

EFFECTS of dynamic stall are regarded as aerodynamically and structurally deleterious. Dynamic stall has been observed on the retreating blades of helicopters, wind turbines, and on rapidly pitching aircraft. Indicators of this stall mechanism are an extension of the linear portion of the lift curve followed by a significant and nonlinear lift overshoot. The vortical structure associated with these effects also induces large pitching-moment fluctuations associated with its advection over the wing surface. Generally, the largest lift overshoot is associated with the dynamic-stall vortex (DSV) located at the midchord position, whereas the largest moment excursion occurs with DSV passage over the wing trailing edge.<sup>1</sup> Experimental evidence suggests that the convection velocity of the DSV is to first-order constant (at approximately  $\frac{1}{3}$  of the freestream) and is independent of pitch rate or airfoil shape.<sup>1</sup> Four mechanisms have been suggested as causative in DSV formation<sup>2</sup>: 1) bursting of the leading-edge laminar separation bubble, 2) transonic flow near the leading edge, 3) separation of the turbulent flow following closure of the laminar separation bubble, and 4) reverse flow near the leading edge stemming from the upstream penetrating reverse layer associated with trailing edge stall.

Received 21 May 2003; revision received 30 May 2003; accepted for publication 2 June 2003. Copyright © 2003 by the authors. Published by the American Institute of Aeronautics and Astronautics, Inc., with permission. Copies of this paper may be made for personal or internal use, on condition that the copier pay the \$10.00 per-copy fee to the Copyright Clearance Center, Inc., 222 Rosewood Drive, Danvers, MA 01923; include the code 0021-8699/04 \$10.00 in correspondence with the CCC.

\*TEES Research Scientist/Lecturer, Aerospace Engineering Department.

<sup>†</sup>Graduate Student, Aerospace Engineering Department. Student Member AIAA.

<sup>‡</sup>Associate Professor, Aerospace Engineering Department. Associate Fellow AIAA.